

# Rapidity and transverse momentum dependence of $\pi^- \pi^-$ Bose-Einstein correlations measured at 20, 30, 40, 80, and 158 A·GeV beam energy

S. Kniege<sup>9,\*</sup>, C. Alt<sup>9</sup>, T. Anticic<sup>21</sup>, B. Baatar<sup>8</sup>, D. Barna<sup>4</sup>, J. Bartke<sup>6</sup>, L. Betev<sup>9,10</sup>, H. Białkowska<sup>19</sup>, A. Billmeier<sup>9</sup>, C. Blume<sup>9</sup>, B. Boimska<sup>19</sup>, M. Botje<sup>1</sup>, J. Bracinik<sup>3</sup>, R. Bramm<sup>9</sup>, R. Brun<sup>10</sup>, P. Bunčić<sup>9,10</sup>, V. Cerny<sup>3</sup>, P. Christakoglou<sup>2</sup>, O. Chvala<sup>15</sup>, J.G. Cramer<sup>17</sup>, P. Csató<sup>4</sup>, N. Darmanov<sup>18</sup>, A. Dimitrov<sup>18</sup>, P. Dinkelaker<sup>9</sup>, V. Eckardt<sup>14</sup>, G. Farantatos<sup>2</sup>, P. Filip<sup>14</sup>, D. Flierl<sup>9</sup>, Z. Fodor<sup>4</sup>, P. Foka<sup>7</sup>, P. Freund<sup>14</sup>, V. Friese<sup>7</sup>, J. Gál<sup>4</sup>, M. Gaździcki<sup>9,12</sup>, G. Georgopoulos<sup>2</sup>, E. Gladysz<sup>6</sup>, K. Grebieszko<sup>20</sup>, S. Hegyi<sup>4</sup>, C. Höhne<sup>13</sup>, K. Kadija<sup>21</sup>, A. Karev<sup>14</sup>, M. Kliemant<sup>9</sup>, V.I. Kolesnikov<sup>8</sup>, T. Kollegger<sup>9</sup>, E. Kornas<sup>6</sup>, R. Korus<sup>12</sup>, M. Kowalski<sup>6</sup>, I. Kraus<sup>7</sup>, M. Kreps<sup>3</sup>, M. van Leeuwen<sup>1</sup>, P. Lévai<sup>4</sup>, L. Litov<sup>18</sup>, B. Lungwitz<sup>9</sup>, M. Makariev<sup>18</sup>, A.I. Malakhov<sup>8</sup>, C. Markert<sup>7</sup>, M. Mateev<sup>18</sup>, B.W. Mayes<sup>11</sup>, G.L. Melcumov<sup>8</sup>, C. Meurer<sup>9</sup>, A. Mischke<sup>7</sup>, M. Mitrovski<sup>9</sup>, J. Molnár<sup>4</sup>, St. Mrówczyński<sup>12</sup>, G. Pála<sup>4</sup>, A.D. Panagiotou<sup>2</sup>, D. Panayotov<sup>18</sup>, A. Petridis<sup>2</sup>, M. Pikna<sup>3</sup>, L. Pinsky<sup>11</sup>, F. Pühlhofer<sup>13</sup>, J.G. Reid<sup>17</sup>, R. Renfordt<sup>9</sup>, A. Richard<sup>9</sup>, C. Roland<sup>5</sup>, G. Roland<sup>5</sup>, M. Rybczyński<sup>12</sup>, A. Rybicki<sup>6,10</sup>, A. Sandoval<sup>7</sup>, H. Sann<sup>7</sup>, N. Schmitz<sup>14</sup>, P. Seyboth<sup>14</sup>, F. Siklér<sup>4</sup>, B. Sitar<sup>3</sup>, E. Skrzypczak<sup>20</sup>, G. Stefanek<sup>12</sup>, R. Stock<sup>9</sup>, H. Ströbele<sup>9</sup>, T. Susa<sup>21</sup>, I. Szentpétery<sup>4</sup>, J. Sziklai<sup>4</sup>, T.A. Trainor<sup>17</sup>, D. Varga<sup>4</sup>, M. Vassiliou<sup>2</sup>, G.I. Veres<sup>4,5</sup>, G. Vesztergombi<sup>4</sup>, D. Vranić<sup>7</sup>, A. Wetzler<sup>9</sup>, Z. Włodarczyk<sup>12</sup>, I.K. Yoo<sup>16</sup>, J. Zaranek<sup>9</sup>, J. Zimányi<sup>4</sup>

(NA49 Collaboration)

<sup>1</sup>NIKHEF, Amsterdam, Netherlands.

<sup>2</sup>Department of Physics, University of Athens, Athens, Greece.

<sup>3</sup>Comenius University, Bratislava, Slovakia.

<sup>4</sup>KFKI Research Institute for Particle and Nuclear Physics, Budapest, Hungary.

<sup>5</sup>MIT, Cambridge, USA.

<sup>6</sup>Institute of Nuclear Physics, Cracow, Poland.

<sup>7</sup>Gesellschaft für Schwerionenforschung (GSI), Darmstadt, Germany.

<sup>8</sup>Joint Institute for Nuclear Research, Dubna, Russia.

<sup>9</sup>Fachbereich Physik der Universität, Frankfurt, Germany.

<sup>10</sup>CERN, Geneva, Switzerland.

<sup>11</sup>University of Houston, Houston, TX, USA.

<sup>12</sup>Institute of Physics Świ etokrzyska Academy, Kielce, Poland.

<sup>13</sup>Fachbereich Physik der Universität, Marburg, Germany.

<sup>14</sup>Max-Planck-Institut für Physik, Munich, Germany.

<sup>15</sup>Institute of Particle and Nuclear Physics, Charles University, Prague, Czech Republic.

<sup>16</sup>Department of Physics, Pusan National University, Pusan, Republic of Korea.

<sup>17</sup>Nuclear Physics Laboratory, University of Washington, Seattle, WA, USA.

<sup>18</sup>Atomic Physics Department, Sofia University St. Kliment Ohridski, Sofia, Bulgaria.

<sup>19</sup>Institute for Nuclear Studies, Warsaw, Poland.

<sup>20</sup>Institute for Experimental Physics, University of Warsaw, Warsaw, Poland.

<sup>21</sup>Rudjer Boskovic Institute, Zagreb, Croatia.

\* parallel talk presented at Quark Matter 2004

**Abstract:** Preliminary results on  $\pi^- \pi^-$  Bose-Einstein correlations in central Pb+Pb collisions measured by the NA49 experiment are presented. Rapidity as well as transverse momentum dependence of the HBT- radii are shown for collisions at 20, 30, 40, 80, and 158 A·GeV beam energy. Including results from AGS and RHIC experiments only a weak energy dependence of the radii is observed. Based on hydrodynamical models parameters like lifetime and geometrical radius of the source are derived from the dependence of the radii on transverse momentum.

## 1. Introduction

The objective of HBT analysis is to obtain information about the spatial and temporal evolution of high energy collisions by means of two-particle Bose-Einstein correlations. Two particle correlations in general lead to a difference between the product of single-particle distributions  $P(1)P(2)$  and the corresponding two-particle distribution  $P(1,2)$ . The symmetrisation of the two particle wave function for bosons results in an enhancement of pairs with small relative momenta of the particles. We construct the correlation function  $C_2(q)$  as the normalised ratio of a distribution of the momentum difference of true pairs  $S(q)$  and a mixed event background distribution  $B(q)$ :

$$C_2(q) = \frac{P(1,2)}{P(1)P(2)} = N \cdot \frac{S(q)}{B(q)}. \quad (1)$$

Due to space-momentum correlations in an expanding source the measured correlations do not reflect the whole extension of the source. This enables us to study the space time evolution of the source by analysing the correlation function in different bins of mean transverse momentum  $k_t$  and pair rapidity  $Y$ :

$$k_t = \frac{1}{2} |\vec{p}_{t,1} + \vec{p}_{t,2}| \quad , \quad Y = \frac{1}{2} \log \left( \frac{E_1 + E_2 + p_{z,1} + p_{z,2}}{E_1 + E_2 - p_{z,1} - p_{z,2}} \right). \quad (2)$$

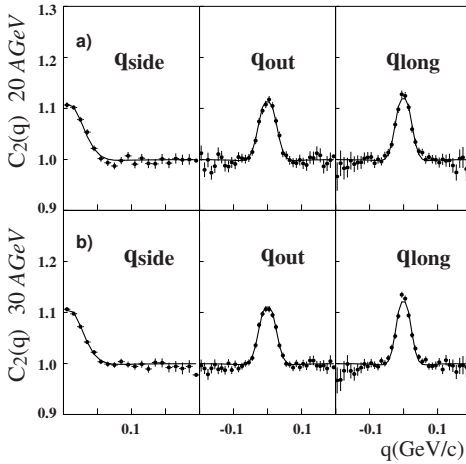


**Figure 1 :** Projections of the 3-dimensional correlation function and the corresponding fits of eqn.4 (solid lines) onto the components  $q_{side}$ ,  $q_{out}$ , and  $q_{long}$  for 20 (a) and 30 A·GeV (b) in the  $k_t$ -bin (0.0-0.1) GeV/c at midrapidity. Projection range : 0.03 GeV/c.

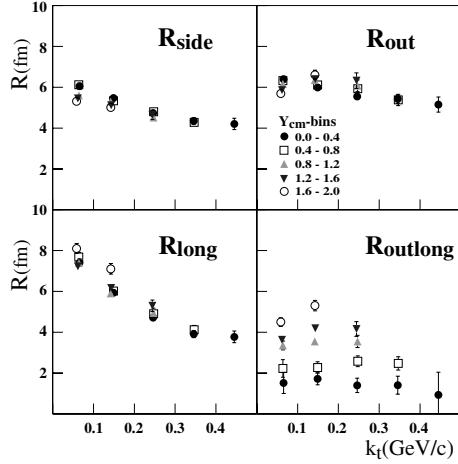


**Figure 2 :** Rapidity and transverse momentum dependence of the HBT-radii  $R_{side}$ ,  $R_{out}$ ,  $R_{long}$  and  $R_{outlong}$  for 30 A·GeV beam energy.

## 2. Experiment and Analysis

NA49 [1] is a fixed target experiment located at the CERN SPS which comprises four large-volume Time Projection Chambers (TPC). A zero degree calorimeter at the downstream end of the experiment is used to trigger on the centrality of the collisions. The data presented here correspond to the 7.2% most central events for 20, 30, 40, and 80 A·GeV and the 10% most central events for 160 A·GeV. Measuring the specific energy loss  $dE/dx$  of charged particles in the gas of the TPC's allows for particle identification with a resolution of 3-4%. However, due to ambiguities in particle identification by specific energy loss measurements in certain regions of phase space negative hadrons rather than identified negative pions are used for the analysis. The limited two track resolution of the detector is taken into account by rejecting pairs with an average distance of particles less than 2.0 cm in the signal- as well as in the background distribution. Following the approach of Pratt and Bertsch [2] the momentum difference is decomposed into a component parallel to the beam axis  $q_{long}$  and two components in the transverse plane  $q_{out}$  and  $q_{side}$ . Where  $q_{out}$  is defined parallel, and  $q_{side}$  perpendicular to  $k_t$ . The correlation function is parametrised by a gaussian

$$C_2(q)_{th} = 1 + \lambda \cdot \exp(-R_o^2 q_o^2 - R_s^2 q_s^2 - R_l^2 q_l^2 - 2R_{ol}^2 q_o q_l) \quad (3)$$

and the parameters  $R_{out}$ ,  $R_{side}$ ,  $R_{long}$ ,  $R_{outlong}$ , and  $\lambda$  are determined by a fit to the measured correlation function. The calculations are done in the longitudinal rest frame of the pair (LCMS) where the crossterm  $R_{ol}$  is supposed to vanish at mid rapidity under the assumption of a longitudinally boost invariant expansion [3]. For a chaotic source the parameter  $\lambda$  is expected to be unity and  $C_2(q)_{th}$  should reach the value 2 for  $q \rightarrow 0$ . However, due to contaminations of the sample with non-pions and pions from long lived resonances or weak decays, the height of the measured correlation function is reduced. To account for this effect we weight  $C_2(q)_{th}$  by a factor  $p$  determined by simulations, which corresponds to the fraction of correlated pairs in the sample. Another major effect determining the shape of the measured correlation function is the Coulomb interaction of charged particles. It is accounted for by a factor  $W(q, r_m)$ , so that the final fit-function is given by:

$$C_2(q)_f = p \cdot (C_2(q)_{th} \cdot W(q, r_m)) + (1 - p). \quad (4)$$

The Coulomb-weight  $W(q, r_m)$  depends on the momentum difference  $q$  as well as on the mean pair separation  $r_m$  of the particles in the source. It is calculated using a method derived by Sinyukov *et al* [4] which also provides a prescription to derive the value of  $r_m$  from the extracted source parameters  $R_{out}$ ,  $R_{side}$ , and  $R_{long}$ . We therefore determine the source parameters as well as the value of  $r_m$  in an iterative fit-procedure. The sample was divided into 5 bins in  $k_t$  in the range 0.0-0.5 GeV/c. In longitudinal direction the binsize was chosen to be 0.4 (20, 30, 40 A·GeV) and 0.5 (80, 160 A·GeV) units of pair rapidity. An example for the projections of the 3-dimensional correlation function and the corresponding fits is given in Figure 1.

## 3. Results

The data presented are not corrected for momentum resolution. The systematic errors of the radii are about 0.5 fm. Since the Radii are measured in the LCMS only a weak rapidity dependence of  $R_{out}$ ,  $R_{side}$ , and  $R_{long}$  is observed at all energies. However, the finite extension of the source leads to deviations from the expected boost invariant expansion which shows up in an increase of the value of  $R_{outlong}$  with

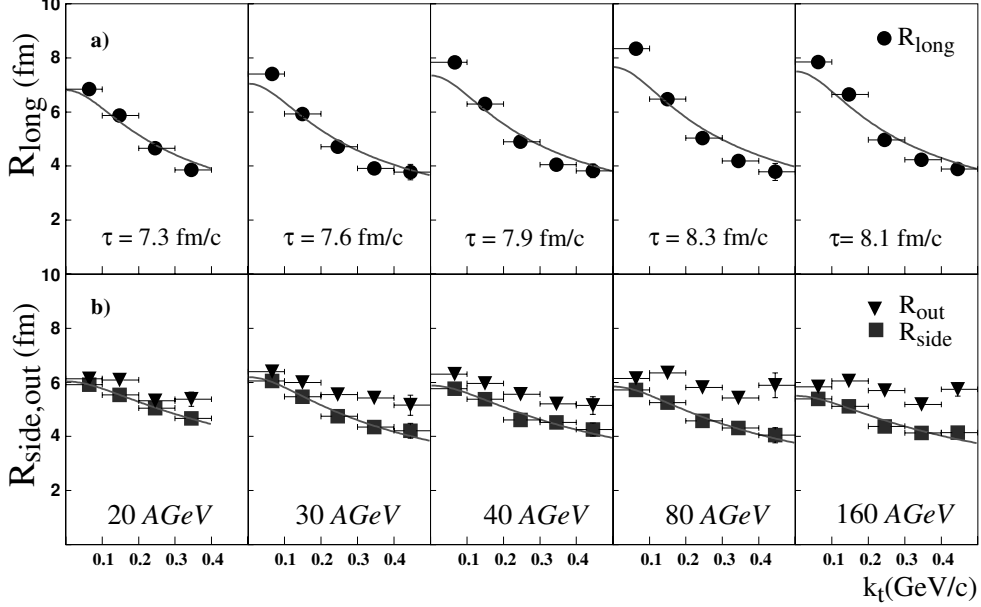


**Figure 3 :**  $k_t$ -dependence of HBT-radii at midrapidity for central Pb-Pb collisions at 20 to 160 A·GeV beam energy as measured by NA49. The solid lines correspond to fits of eqns. 5 and 6 to  $R_{long}$  and  $R_{side}$ , respectively.

increasing rapidity as shown in Figure 2 for 30 A·GeV beam energy. Longitudinal and transverse expansion lead to a reduction of the correlation-lengths with  $k_t$ , which is partly compensated by a superimposed thermal velocity-field. In case of a Bjorken scenario the  $k_t$ -dependence of  $R_{long}$  reflects the life time of the source [5]:

$$R_{long} = \tau_f (T_f/m_t)^{1/2} \quad , \quad m_t = (m_\pi^2 + k_t^2)^{1/2}. \quad (5)$$

Under the assumption of a freezeout temperature  $T_f = 120$  MeV a slight increase of life time with energy is observed (Figure 3.a). Assuming a hydrodynamical model with transverse expansion characterized by a linear flow profile with rapidity  $\eta_f$ , the transverse geometrical radius  $R_{geo}$  of the source can be extracted from the  $k_t$ -dependence of  $R_{side}$  [6]:

$$R_{side} = R_{geo}/(1 + m_t \cdot \eta_f^2/T_f)^{1/2}. \quad (6)$$

From fits to the data in Figure 3.b we obtain values for the geometrical radius  $R_{geo}$  of about 7-9 fm, but we do not observe a significant energy dependence. Another important parameter is the emission duration of the source which can be determined by [7]:

$$\Delta\tau^2 = \frac{1}{\beta_t^2} (R_{out}^2 - R_{side}^2) \quad , \quad \beta_t \approx \frac{k_t}{m_t}. \quad (7)$$

As seen in the panels of Figure 3.b the difference between  $R_{out}$  and  $R_{side}$  is positive for all energies and the emission duration comes out to be about 3-4 fm/c.

In summary the NA49-results only show a weak energy dependence of the extracted HBT-radii and of the corresponding source parameters at SPS energies. This trend persists if we include results from AGS and RHIC experiments as shown in Figure 4. We only see a slight rise of  $R_{long}$  starting at SPS energies indicating an increase of

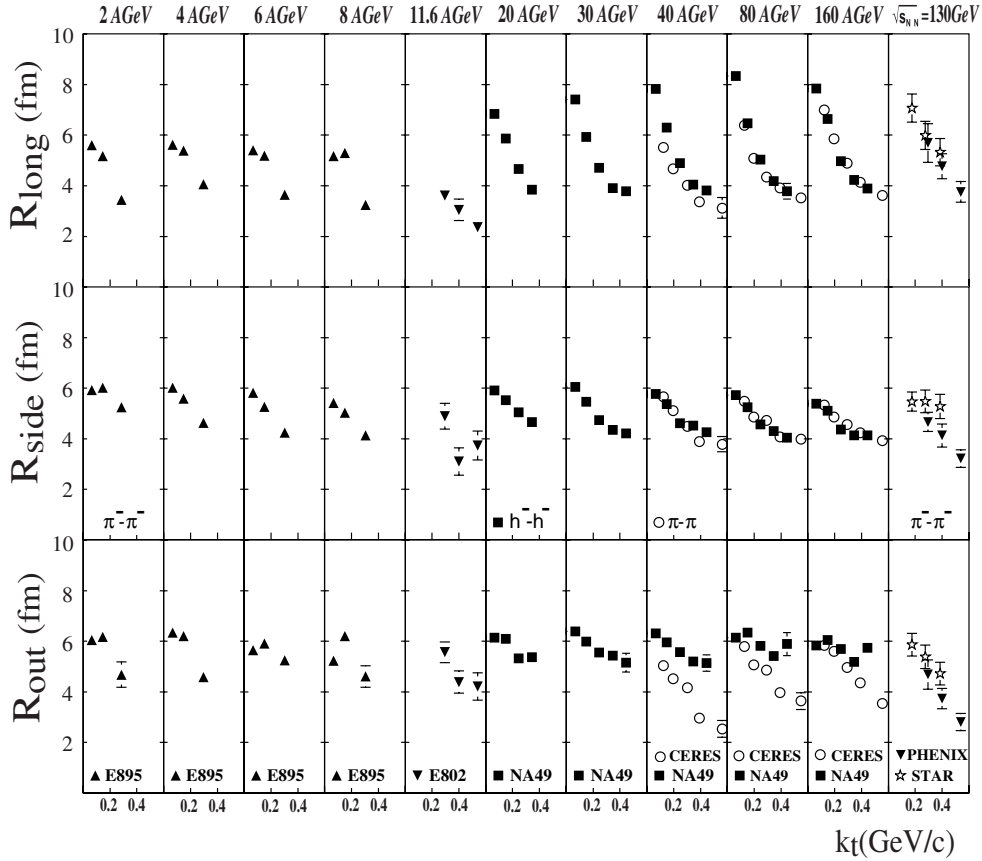


**Figure 4 :** Energy- and  $k_t$ -dependence of the radii  $R_{long}$ ,  $R_{side}$ , and  $R_{out}$  for central Pb+Pb(Au+Au) collisions from AGS to RHIC experiments measured near midrapidity.

the life time of the source.  $R_{side}$  and  $R_{out}$  remain approximately constant over the whole energy range.

**Acknowledgements:** This work was supported by the US Department of Energy Grant DE-FG03-97ER41020/A000, the Bundesministerium für Bildung und Forschung, Germany, the Polish State Committee for Scientific Research (2 P03B 130 23, SPB/CERN/P-03/Dz 446/2002-2004, 2 P03B 04123), the Hungarian Scientific Research Foundation (T032648, T032293, T043514), the Hungarian National Science Foundation, OTKA, (F034707), the Polish-German Foundation, and the Korea Research Foundation Grant (KRF-2003-070-C00015).

## REFERENCES

- [1] S. V. Afanasiev *et al* (NA49 Collaboration), Phys. Rev. **C 66** (2002) 054902
- [2] S. Pratt, Phys. Rev. **C 33** (1986) 72
- [3] U. Heinz and U. Wiedemann, Phys. Rept. **319** (1999) 145
- [4] Y. M. Synukov *et al*, Phys. Lett. **B 432** (1998) 248
- [5] A. Makhlin and Y. M. Synukov, Z. Phys. **C 39** (1988) 69
- [6] S. Chapman, J. Nix and U. Heinz, Phys. Rev. **C 52** (1995) 2694
- [7] U. Heinz *et al*, Phys. Lett. **B 382** (1996) 181